ACS APPLIED MATERIALS & INTERFACES

Research Article

www.acsami.org

Tuning the Observability of Surface Plasmon in Silica–Gold Raspberry Shaped Nanoparticles Using Cuprous Oxide Shell

Himanshu Tyagi,[†] Jeotikanta Mohapatra,[‡] Ajay Kushwaha,[†] and Mohammed Aslam*[,†]

[†]National Centre for Photovoltaic Research and Education (NCPRE) and Department of Physics, Indian Institute of Technology Bombay, Powai, Mumbai-400076, India

[‡]Centre for Research in Nanotechnology and Science (CRNTS), Indian Institute of Technology Bombay, Powai, Mumbai-400076, India

Supporting Information

ABSTRACT: A raspberry shaped silica–gold nanoparticle system has been coated with a cuprous oxide shell using a simple wet chemical approach. The optical properties of such particles depend on thin dielectric shell material, and we calculate far-field scattering and extinction of cuprous oxide coated silica–gold composite. In accordance with our theoretical findings, for ultrasmall gold nanoparticles (AuNPs < 5 nm) attached over silica, the localized surface plasmon resonance (LSPR) peak is completely suppressed after Cu_2O coating. The cloaking (nonobservability) of the LSPR peak in extinction spectra has been explained via calculation of contribution from absorbance (<10%) and scattering (>90%) in the composite nanostructure. For larger particles (>5 nm), the traditional red-shift of the plasmon peak (from 532 to 588 nm) is still significant due to the large dielectric constant (approx. 8.0 @ 600 nm) of cuprous oxide (Cu_2O) coating. A complete and controlled suppression of LSPR in small sized gold nanoparticles due to high dielectric refractory oxide shell could play a significant role in plasmon derived applications.

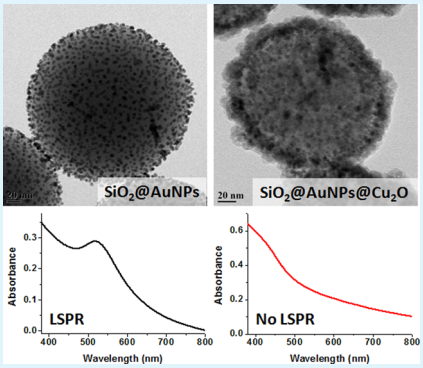

KEYWORDS: *gold nanoparticles, cuprous oxide, core–shell, plasmon, cloaking, dielectric constant*

INTRODUCTION

Metal-semiconductor hetero-nanostructures are very interesting from the viewpoint of optical and catalytic properties.[1−7] It has been shown that gold nanoparticles (AuNPs) show intense plasmon absorption in visible range which is very sensitive to dielectric properties of surrounding media. Recently, there have been reports in literature which discuss growth of cuprous oxide shell around AuNPs and red shift in plasmon of gold nanoparticles when coated with Cu_2O.[8−11] However, primary focus has been on Cu_2O coating of AuNP of sizes larger than 15 nm, and such composites show plasmon peak in wavelength range of 600−1000 nm with varying thickness of Cu_2O coating. This significant red-shift in plasmon peak of gold nanoparticles occurs due to high dielectric constant (>7) of cuprous oxide shell, and as the Cu_2O shell thickness increases, the localized surface plasmon resonance (LSPR) peak is found to shift in NIR region. Moreover, the intensity of LSPR for larger AuNP increases with thickness of Cu_2O shell since scattering becomes a significant contribution to LSPR. An intense and sensitive LSPR is an attractive feature for surface enhanced Raman spectroscopy (SERS) and sensing applications.[12,13] In accordance with the observations of other research groups,[8−10] a trend of red-shifted and more intense plasmon band after a dielectric overcoat should be observed irrespective of the size of AuNPs. We investigate the effect of Cu_2O coating around small (<5 nm) AuNPs (attached over silica) and find the plasmon is suppressed instead. The absence or presence of plasmon (in extinction spectra of composite) is found to be a size dependent phenomenon, and a plasmon band is seen when the AuNP size is above 5 nm. Thus, the Cu_2O shell instead leads to nonobservability of the LSPR peak, and we attribute the phenomenon to scattering from the Cu_2O shell over silica–gold raspberries.[14,15] We corroborate our experimental results with Mie calculations, and modeled far-field optical response indicates a plasmon suppression for small AuNP case. An increase in imaginary dielectric constant values of Cu_2O in the wavelength regime below 600 nm could also have been an apparent suspect for the suppression of the plasmon in silica@AuNP@Cu_2O (SAC) nanostructures. However, through Mie calculations,[16] we show that increase in imaginary dielectric function marginally affects the absorbance component (Q_{abs} < 0.01) of extinction (Q_{ext} > 0.1) at wavelengths > 500 nm. Since the scattering component is dominant (Q_{scat} > 0.1) and imaginary dielectric function does not play any role (at wavelengths > 500 nm), the absence of LSPR could not be due to the imaginary part of the dielectric function of Cu_2O. The nonobservance of the LSPR peak is thus related to the absence of LSPR in scattering from the nanostructure.

Received: May 21, 2013
Accepted: November 15, 2013
Published: November 15, 2013

EXPERIMENTAL SECTION

Materials. Gold trichloride ($AuCl_3$, Sigma Aldrich), tetraethyl orthosilicate (TEOS, SD Fine-Chem Limited (SDFCL)), ammonia solution (30%, Merck Millipore), (3-aminopropyl)trimethoxysilane (APTMS, Sigma Aldrich), sodium borohydride ($NaBH_4$, SDFCL), sodium hydroxide (NaOH, SDFCL), hydrochloric acid (HCl, 37%, Merck Millipore), copper(II) nitrate trihydrate ($Cu(NO_3)_2{\cdot}3H_2O$, SDFCL), polyvinylpyrrolidone (PVP K-30, SDFCL), hydrazine hydrate (80% in water, SDFCL), ethanol (HPLC grade, Commercial Alcohols), and 2-propanol (Merck Millipore) were used. All chemicals were used as-is without any further purification.

Procedure. Silica nanoparticles of 130 nm diameter were prepared using a modified Stober process.[17] Further, these silica particles (100 mg) are amine-functionalized by stirring them overnight in an ethanolic solution (30 mL) of APTMS (0.3 mL) followed by heating (70 °C) under argon atmosphere. The functionalized silica particles are centrifuged out (5000 rpm), and excess APTMS is removed by repeated centrifugation and redispersion (in ethanol) process. The clean amine functionalized silica particles so obtained are dried in argon atmosphere.

Gold nanoparticles of 3−7 nm diameter were synthesized using sodium borohydride as reducing agent.[18] A solution (sol.A) containing 50 mM concentration of $AuCl_3$ and HCl each is prepared in Millipore water (resistivity = 18.2 MΩ). Another solution (sol.B) containing 50 mM concentration of $NaBH_4$ and NaOH each is also prepared using Millipore water. Later, 0.1 mL from sol.A is diluted in 10 mL of deionized water and then y mL of sol.B is added to it while stirring at room temperature conditions. The mixture is vigorously stirred for 2 min followed by heating the sol at 70 °C for 3 min so as to remove the hydrogen bubbles formed due to sodium borohydride. The size of gold nanoparticles depends on the value of y; for y = 300, 425, 575, 650, and 1100 μL, we obtain AuNPs of diameter 3, 4, 5, 6, and 7 nm, respectively. Gold nanoparticles of diameter 10 nm were synthesized using the standard Turkevich method[19] by adding 2 mL of trisodium citrate (1 wt % in water) to 38 mL of $HAuCl_4$ (0.5 mM) solution boiling at 100 °C. The boiling was continued for 15 min, and the appearance of red color indicates formation of AuNPs.

To attach AuNPs (3−7 nm) over the silica nanoparticles surface, 20 mg of functionalized silica is added to 10 mL of AuNP solution followed by 5 min sonication. The mixture is left undisturbed for 15 min, and thereafter, we clean the obtained SA product via centrifugation and redispersion in ethanol. For attaching 10 nm AuNPs over silica, 24 mg of functionalized silica is added to 40 mL of AuNP solution and the rest of the procedure is same as that used for coating 3−7 nm AuNPs over silica.

Copper(I) oxide coating over SA systems is achieved by adding 10 mg of SA (dispersed in 10 mL ethanol) to a solution containing 0.0242 g of cupric nitrate and 0.2 g of PVP in propanol (60 mL). To this solution 0.04 g of NaOH dissolved in 5 mL of propanol is added. After addition of NaOH, 0.4 mL of hydrazine (35 wt %) is added dropwise to above mixture while stirring continuously (800 rpm). After 15 min of stirring, we centrifuge out the resulting particles which are further cleaned via redispersion and centrifugation process. Thin films of particles were prepared via spin-casting the particles (1 mg/mL) on glass substrate. The glass substrates were cleaned using piranha mixture prior to the deposition of particles. **Caution**: *Piranha mixture is very corrosive and boils upon mixing.*

The extinction of particles (dispersed in ethanol) and transmission/reflection spectra of thin films were measured using a PerkinElmer Lambda 950 UV−vis spectrometer, while transmission electron microscopy (TEM) imaging and selected area electron diffraction (SAED) were performed with a JEOL 2100F FEG transmission electron microscope.

RESULTS AND DISCUSSION

The gold nanoparticles of sizes 3, 4, 5, 6, 7 (std. dev. < 1 nm), and 10 nm (std. dev. = 1.5 nm) show plasmon peak positions at 508, 510, 511, 512, 519, and 521 nm, respectively, confirming the size control of nanoparticles.[18,19] We used a sodium borohydride based process[18] to synthesize gold nanoparticles (3−7 nm size range) in an aqueous medium, and due to charge transfer from borohydride anions to AuNPs, plasmon peak is shifted to wavelengths below 520 nm.[20] We see a dense attachment of gold nanoparticles over amine functionalized silica nanospheres of diameter 130 nm (Figure 1).[21] TEM

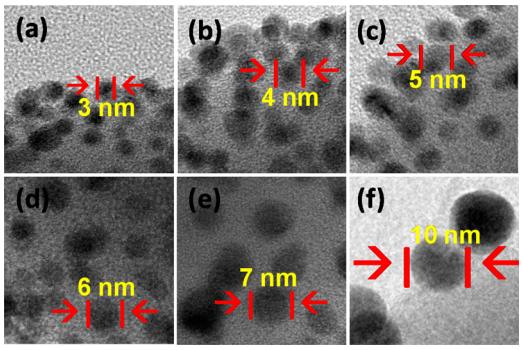

Figure 1. High resolution TEM images of SiO_2@AuNP system with AuNPs of diameter (a) 3 nm, (b) 4 nm, (c) 5 nm, (d) 6 nm, (e) 7 nm, and (f) 10 nm.

images (Figure 2) of synthesized nanostructures confirm the SiO_2 coating with AuNPs and a 10 nm thick Cu_2O layer over the SA raspberries. The SAED pattern further confirms the circular rings corresponding to Au planes (200 and 311) and Cu_2O planes (111 and 220), thus suggesting the crystalline nature of the composite (Figure 2f). Cuprous oxide (Cu_2O) was coated onto SA particles via modification of a method reported in literature.[22] The method to coat Cu_2O over SA particles involves use of PVP as a directing agent which assists Ostwald ripening of cuprous oxide nuclei into a shell over SA nanoparticles. It is also very well-known that Cu_2O grows epitaxially over the AuNPs surface due to small lattice mismatch (4.5%).[10] After the first Cu_2O layer nucleation over the AuNP surface, PVP aids further growth of cuprous oxide shell just around the SA nanospheres.[8,23] Further, PVP also acts as a capping agent which prevents oxidation of Cu_2O to CuO.[24,25] A mixed Cu_2O/CuO crystalline phase is undesirable since it alters the dielectric properties of Cu_2O and will thus hinder efforts to determine the effect of Cu_2O shell on SA particles. We tried synthesizing SAC particles without using PVP and found that the copper oxide shell over SA particles was nonuniform and CuO was present in the shell (details in Supporting Information). Thus, use of PVP is necessary to obtain a uniform and homogeneous shell of Cu_2O around SA particles.

The extinction spectra of SA and SAC particles are taken to characterize the effect of cuprous oxide coating on plasmonic properties of gold nanoparticles (Figure 3). For 6.5 and 10 nm AuNPs, the plasmon peak shifts to 578 and 588 nm, respectively. The large shift in plasmon peak is attributed to high refractive index (n) of cuprous oxide (n = 2.7) compared to ethanol (n = 1.36) as surrounding medium of AuNPs. For AuNPs of diameter less than 5 nm coated with cuprous oxide, the plasmon peak is highly suppressed and disappears if AuNP size is <4 nm (Figure 3b). The absorption coefficient of Cu_2O is ~2×10^3 cm^{-1} at 580 nm wavelength (i.e., near to plasmon wavelength for SAC composites) and for a 10 nm thick Cu_2O layer absorbance is expected to be 0.002.[26] Such a low absorbance for 10 nm thick Cu_2O film implies that it has almost 99.5% transmittance, and thus, the electric field of incident

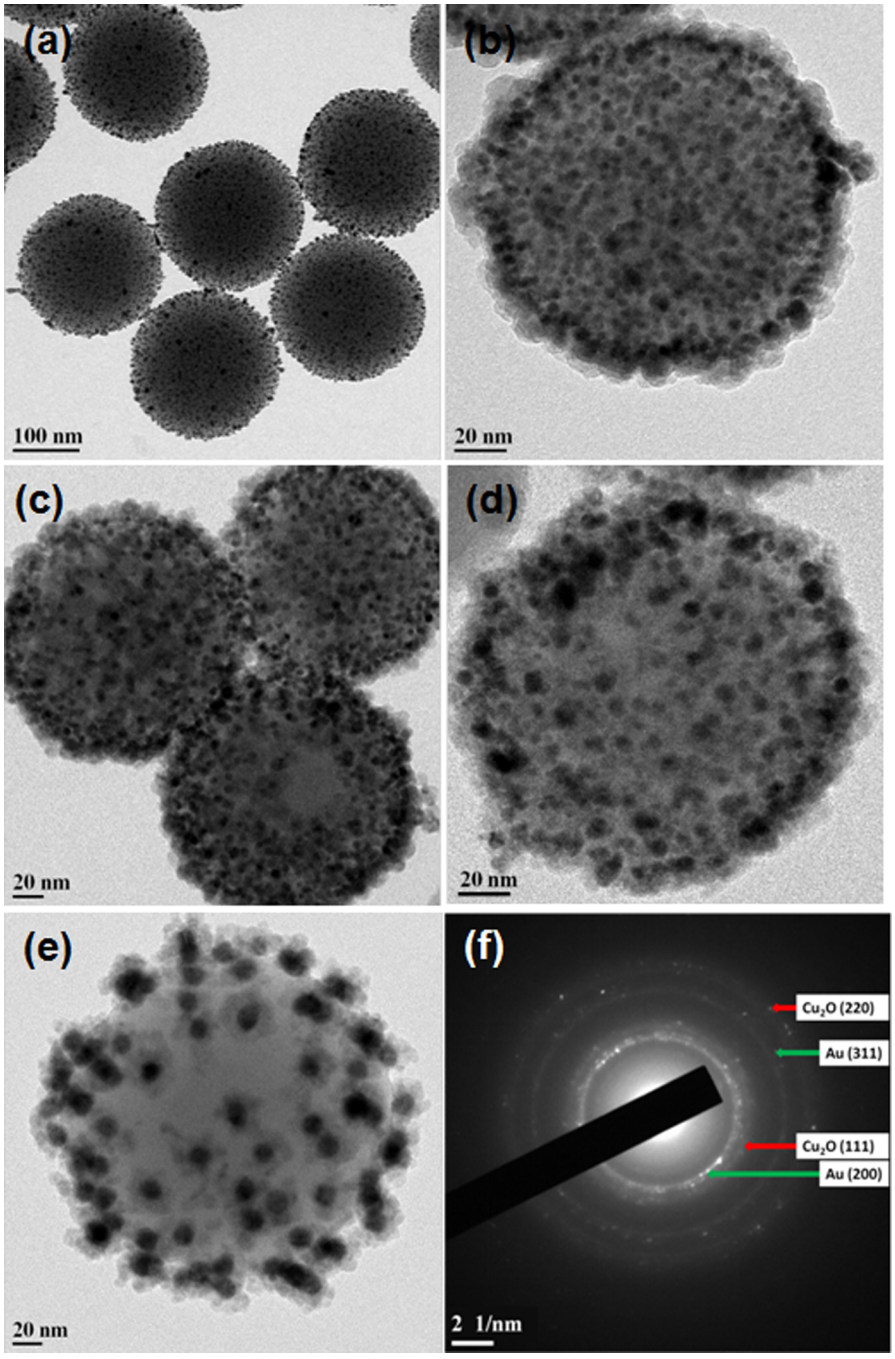

Figure 2. TEM images of (a) SiO_2@AuNP system with AuNPs of diameter = 3 nm, and SiO_2@AuNP system coated with 10 nm of Cu_2O layer, with AuNP size being (b) 3 nm (inset shows the 10 nm thick Cu_2O layer), (c) 5 nm, (d) 7 nm, and (e) 10 nm. (f) TEM diffraction pattern of silica@AuNP@Cu_2O composite with AuNP size 10 nm.

wavelengths will reach AuNPs inside the Cu_2O shell. The negligible absorbance of the Cu_2O coat thus rules out the possibility of nonabsorbance of plasmon due to thickness of cuprous oxide. We investigate whether nonobservance of the plasmon peak is related to imaginary dielectric function of cuprous oxide or large scattering expected from particles which have dimensions comparable to incident wavelength. The imaginary dielectric function of cuprous oxide has negligibly small values at wavelengths above 600 nm, and thus, cuprous oxide is predominantly nonconductor at wavelengths above 600 nm.[26] The imaginary part becomes significant for wavelengths below 600 nm and the nature of cuprous oxide is thus semiconducting for wavelengths below 600 nm. Various studies have shown that when we have a semiconducting media surrounding a plasmonic particle, there can be delocalization of free electrons of AuNPs at the semiconductor−AuNP interface.[27,28] The delocalization of electrons results in lesser availability of free electrons on AuNPs which tends to suppress the plasmon peak. An increase in imaginary part implies an increase in conductivity of cuprous oxide and thus the plasmon peak in wavelength range below 600 nm should be suppressed.[16] However, the plasmon peak is not seen in calculated extinction even after assuming imaginary part of dielectric function of cuprous oxide to be zero in wavelength range of the

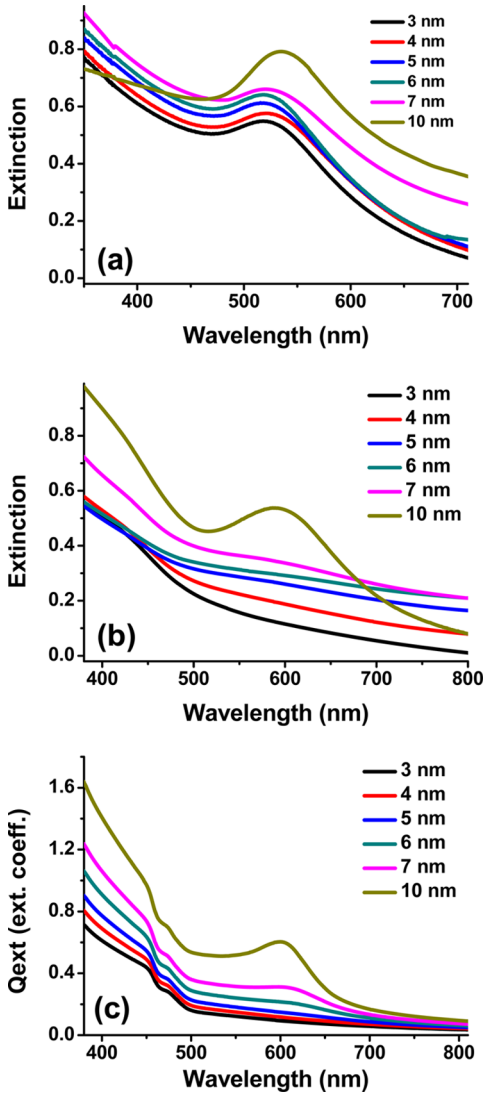

Figure 3. Experimental UV−vis spectra showing plasmon peaks for (a) SiO_2@AuNPs systems with different AuNP diameters (3−10 nm), (b) complete suppression of plasmon peak after Cu_2O shell formation over SiO_2@AuNPs systems with AuNP diameter < 5 nm, and (c) calculated extinction of Cu_2O coated SiO_2@AuNPs systems shows plasmon peak suppression for AuNP size < 5 nm.

interest (Figure 4a). Hence, the imaginary dielectric part of Cu_2O is not a factor contributing to nonobservance of the plasmon peak. As the total diameter of composite nanostructures is above 130 nm, scattering is expected to contribute significantly to observed extinction spectra. We calculate the contribution of scattering and absorbance to extinction via Mie solution for a core−shell problem. The system can be easily and efficiently modeled by considering silica sphere core (diameter = 130 nm) surrounded by a shell with dielectric response similar to that of an AuNP@Cu_2O system. We calculate the dielectric function ($\varepsilon(R, \omega)$) of AuNPs of various radii (R) at various frequencies ω using[29]

$$\varepsilon(R, \omega) = \varepsilon_{\text{bulk}}(\omega) + \frac{{\omega_p}^2}{\omega(\omega + i\tau^{-1})} - \frac{{\omega_p}^2}{\omega(\omega + i\tau^{-1} + iv_F/R)}$$

where $\varepsilon_{\text{bulk}}(\omega)$ is the dielectric function of bulk gold calculated by Johnson and Christy[30] and

$$\hbar\omega_p = 9 \text{ eV}; \quad \hbar\tau^{-1} = 0.05 \text{ eV}$$

Since our system consists of AuNP supported on silica and coated with cuprous oxide shell, we take average of dielectric function of Cu_2O and silica to evaluate the dielectric function of AuNP@Cu_2O system using the Mie expression for a core−shell:[16,20]

$$\varepsilon_{\text{Au-Cu}} = [(\varepsilon_{\text{shell}} - \varepsilon_m)(\varepsilon_{\text{core}} - 2\varepsilon_{\text{shell}}) + (1 - g)(\varepsilon_{\text{core}} - \varepsilon_{\text{shell}})(\varepsilon_m + 2\varepsilon_{\text{shell}})] / [(\varepsilon_{\text{shell}} + 2\varepsilon_m)(\varepsilon_{\text{core}} + 2\varepsilon_{\text{shell}}) + (1 - g)(2\varepsilon_{\text{shell}} - 2\varepsilon_m)(\varepsilon_{\text{core}} - \varepsilon_{\text{shell}})]$$

We utilized the so obtained average dielectric function in Mie expression for a core shell with silica as core and AuNP@Cu_2O as shell material.[21] The extinction calculated in such a model agrees fairly well with the experimentally observed UV−vis response of SAC systems (Figure 3b and c). The model is able to predict the low or no observability of plasmon peak with a smaller sized AuNP as well as the plasmon peak position shift of composite core−shell system. Our calculations show that for core−shell with 3 nm AuNP diameter, scattering dominates and the value of absorbance is very small at wavelengths greater than 500 nm (Figure 4d). Since, the scattering component does not show plasmon band, no band is observed in extinction either. With an increase in AuNP diameter, the absorbance of composite increases and its contribution to extinction becomes significant (Figure 4e and f). Hence, for AuNPs with diameter greater than 5 nm, we observe a LSPR band in extinction spectra as well. The details of Mie scattering calculations can be found in the Supporting Information.

We calculate extinction properties of AuNP@Cu_2O system and compare them to SAC properties so as to highlight the importance of the silica core in nonobservability of the plasmon peak in SA3C nanoparticles. The calculations indicate that a single AuNP (3 nm) with 10 nm Cu_2O shell will show a LSPR peak, although the plasmon peak in extinction is suppressed and would have (along with shifting of LSPR from 520 to 696 nm position due to high refractive index of Cu_2O) lower extinction in comparison to plasmon peak of a bare AuNP (Figure 5). It must be noted that contribution of absorption to extinction is larger than the contribution from scattering. Since the plot of absorption efficiency versus wavelength shows a plasmon peak, LSPR will be seen in extinction. Thus, the role of large sized silica becomes important in the case of SAC structure where contribution of scattering to extinction is considerably larger than the absorption. The absence of a plasmon peak in scattering thus leads to its nonobservability in extinction for the SA3C system.

For many applications and device designs, thin films of nanoparticles are convenient to be used; hence, we measured total transmission and reflection spectra of thin film of SAC particles to evaluate nonobservability of LSPR in thin film configuration. It is found that plasmon peak is absent in both transmittance and reflectance spectra when diameter of AuNP is 3 nm (Figure 6). The transmission shows presence of LSPR at 510 nm for SA3 particles but for SA3C particles LSPR is absent in transmission spectrum. In reflection spectrum, SA3 shows LSPR (as a dip in spectrum) at 538 nm but no LSPR is

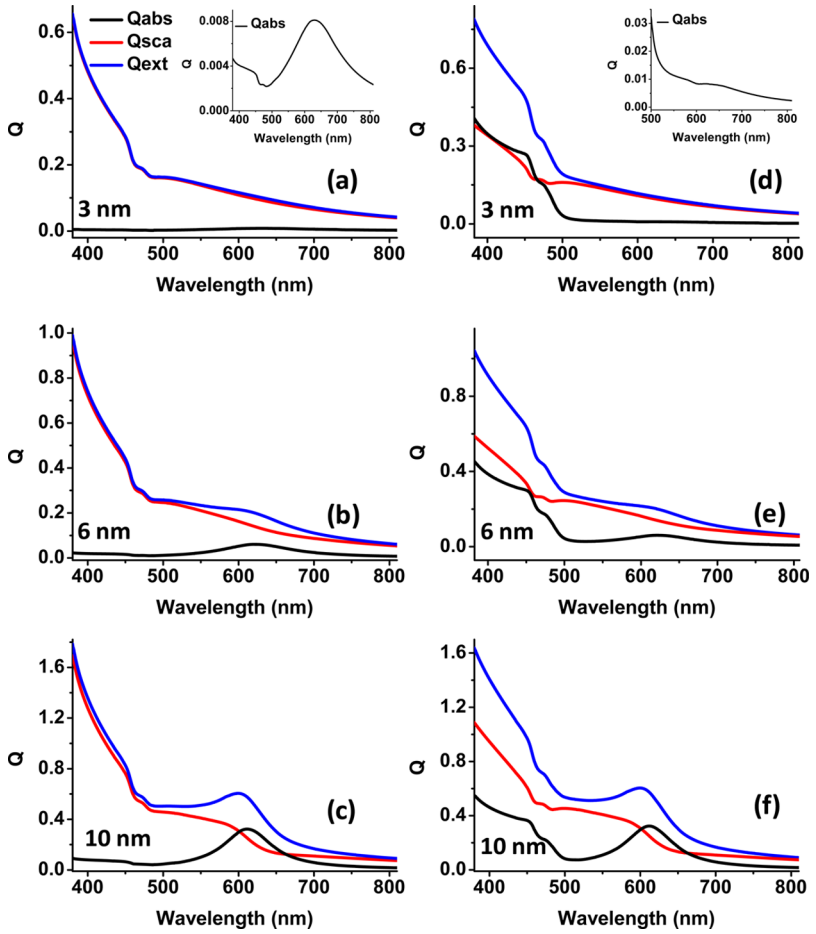

Figure 4. Calculated absorption (black), scattering (red) and extinction (blue) coefficients for silica@AuNP@Cu_2O nanostructures with different AuNP diameters (3, 6, and 10 nm) and ethanol (ε = 1.85) as surrounding medium. The coefficients shown in (a)−(c) have been calculated neglecting imaginary part of dielectric function of Cu_2O while those shown in (d)−(f) have been calculated accounting contribution from imaginary part. Insets in (a) and (d) show the Q_{abs} plots for the two cases showing nearly same extinction values (even though the absorbance peak is much sharper in (a) compared to (d) but Q_{abs} is negligible in both cases to affect overall extinction in the two cases).

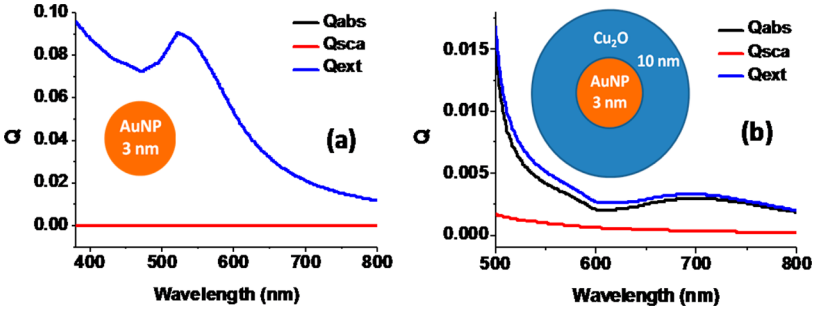

Figure 5. Calculated absorption (black), scattering (red), and extinction (blue) coefficients for (a) AuNP with 3 nm diameter and (b) AuNP@Cu_2O core shell. The curve corresponding to Q_{abs} is not visible in (a); however, Q_{sca} and Q_{abs} are nearly equal for 3 nm AuNPs.

seen for SA3C particles. For composite nanoparticles with gold nanoparticles of 10 nm diameter, LSPR wavelength changes from 528 to 560 nm in transmission after SA10 is overcoated with cuprous oxide; the corresponding LSPR wavelength change in reflection spectra is from 533 to 560 nm. The red-shift of LSPR of SA10 after formation of a Cu_2O shell over it is due to higher refractive index of Cu_2O as compared to air.

It is also interesting to note that LSPR wavelength of same nanoparticle system is different in reflection and transmission mode. The transmission spectra indicates extinction of radiation by nanoparticles while reflection spectra is obtained by measuring back scattered radiations from nanoparticles.[16] Since extinction and scattering LSPR characteristics are not always same, there could be a difference in LSPR wavelengths in two cases.[16,29] Moreover, when the size of the scattering object is comparable to wavelength of incident light, the light is heavily scattered in forward direction.[16] Thus, intensity of back scattered radiation is very small as compared to intensity of forward scattered radiation and instead of a peak corresponding to LSPR, we will see a dip at LSPR wavelength.[31] Since the size of SA and SAC systems are comparable to typical LSPR wavelengths (diameter to LSPR wavelength ratio ~0.25), we

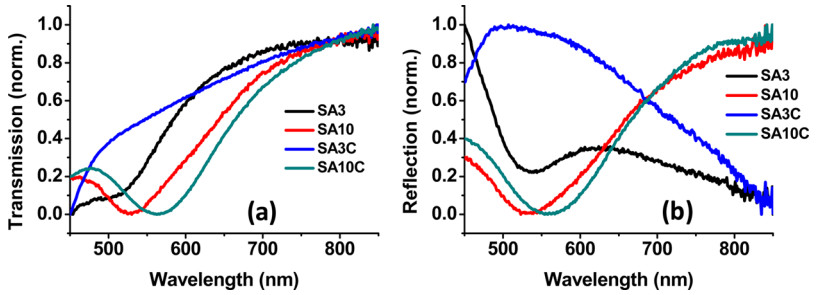

Figure 6. Normalized (a) transmission and (b) reflection spectra for films of silica@AuNP raspberries with and without Cu_2O shell. The diameter of AuNPs is 3 and 10 nm and cleaned glass was used as a substrate. (The data was normalized in [0, 1] range against intensity.)

observe a dip rather than a peak for LSPR in their reflection spectra. For a SA system, spectra will typically show LSPR wavelength similar to case of an individual AuNP in air, with a slight red-shift in LSPR wavelength due to its proximity to silica.[16,21] An individual AuNP in air will show LSPR at larger wavelength in scattering compared to LSPR wavelength in extinction. (Note: Even though scattering from AuNP alone is very less but for silica@AuNP system, scattering is expected to be significant, refer to Figure S3 in the Supporting Information). Hence, we see a difference between plasmonic characteristics in transmission and reflection spectra of SA systems.

For SA10C system in air, Mie calculations indicate that it will show plasmon resonance at 590 and 600 nm in scattering and extinction spectra, respectively; however, the scattering efficiency (0.04) at plasmon resonance is negligible in comparison to absorption efficiency (0.4), and thus, the dip (corresponding to LSPR) in reflected intensity will depend on absorption by particles rather than the scattering (Figure 7).

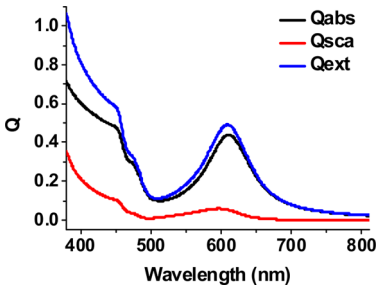

Figure 7. Calculated absorption (black), scattering (red), and extinction (blue) coefficients for silica@AuNP@Cu_2O nanostructure with AuNP diameter of 10 nm and air ($\varepsilon = 1$) as surrounding medium.

Since, absorption heavily dominates scattering for SA10C in an air medium, the LSPR wavelength is the same in reflection and transmission spectra. The difference between calculated and actual spectra (for SA10C) can be attributed to approximation of a continuous shell of AuNP-Cu_2O over silica nanosphere while calculating Q_{ext}, Q_{scat}, and Q_{abs} for the particles. In TEM images of SA10C (Figure 2e), we see individual AuNPs coated with 10 nm thick Cu_2O and not a full coat of Cu_2O over the silica–AuNP system. Hence, comparison of calculated and actual spectra for SA10C is qualitative only.

CONCLUSIONS

We present the suppression of plasmon in 5 nm and smaller size AuNPs (supported on silica) with 10 nm cuprous oxide shell. The plasmon peak is typical and trendy if the diameter of AuNPs is greater than 5 nm. Absence of a plasmon band in dominant scattering spectra and a low value of absorbance are found to be responsible for cloaking of the plasmon band in far-field extinction spectra of SAC nanospheres (when diameter of AuNP is below 5 nm). Our study thus provides a unique way to control and cloak the LSPR peak by tailoring the scattering component of far-field extinction spectrum. We believe that such control would be helpful in designs of antireflection coatings, plasmonic material based solar cells, and cloaking devices.

ASSOCIATED CONTENT

Supporting Information

Details of calculations of far-field response of core–shell nanostructures, large scale TEM images of various nanostructures, and discussion on the role of PVP in synthesis of SAC particles. This material is available free of charge via the Internet at http://pubs.acs.org.

AUTHOR INFORMATION

Corresponding Author

*E-mail: m.aslam@iitb.ac.in.

Author Contributions

The manuscript was written through contributions of all authors. All authors have given approval to the final version of the manuscript.

Notes

The authors declare no competing financial interest.

ACKNOWLEDGMENTS

We thank Professor Kailash C. Rustagi (Department of Physics, IIT Bombay) for discussion on UV–vis spectroscopy results. We also thank CRNTS, IIT Bombay for providing FEG-TEM facility. We gratefully acknowledge the Industrial Research and Consultancy Center (IRCC) of IIT Bombay, Council of Scientific and Industrial Research (CSIR, New Delhi), and National Center for Photovoltaic Research and Education (NCPRE-project funded by MNRE, the Government of India) for the financial support of this work.

ABBREVIATIONS

LSPR = localized surface plasmon resonance; AuNP = gold nanoparticle; SA(n) = silica@AuNP with n as diameter of AuNPs; SA(n)C = silica@AuNP@Cu_2O with n as diameter of AuNPs

REFERENCES

(1) Bardhan, R.; Grady, N. K.; Ali, T.; Halas, N. J. *ACS Nano* **2010**, *4*, 6169–6179.

(2) Fofang, N. T.; Grady, N. K.; Fan, Z. Y.; Govorov, A. O.; Halas, N. J. *Nano Lett.* **2011**, *11*, 1556−1560.
(3) Kobayashi, Y.; Nonoguchi, Y.; Wang, L.; Kawai, T.; Tamai, N. *J. Phys. Chem. Lett.* **2012**, *3*, 1111−1116.
(4) Kuo, C. H.; Yang, Y. C.; Gwo, S.; Huang, M. H. *J. Am. Chem. Soc.* **2011**, *133*, 1052−1057.
(5) Pan, Y.; Deng, S.; Polavarapu, L.; Gao, N.; Yuan, P.; Sow, C. H.; Xu, Q. *Langmuir* **2012**, *28*, 12304−12310.
(6) Georgekutty, R.; Seery, M. K.; Pillai, S. C. *J. Phys. Chem. C* **2008**, *112*, 13563−13570.
(7) Zheng, Y. H.; Chen, C. Q.; Zhan, Y. Y.; Lin, X. Y.; Zheng, Q.; Wei, K. M.; Zhu, J. F. *J. Phys. Chem. C* **2008**, *112*, 10773−10777.
(8) Zhang, L.; Blom, D. A.; Wang, H. *Chem. Mater.* **2011**, *23*, 4587−4598.
(9) Liu, D. Y.; Ding, S. Y.; Lin, H. X.; Liu, B. J.; Ye, Z. Z.; Fan, F. R.; Ren, B.; Tian, Z. Q. *J. Phys. Chem. C* **2012**, *116*, 4477−4483.
(10) Zhang, L.; Jing, H.; Boisvert, G.; He, J. Z.; Wang, H. *ACS Nano* **2012**, *6*, 3514−3527.
(11) Wang, W. C.; Lyu, L. M.; Huang, M. H. *Chem. Mater.* **2011**, *23*, 2677−2684.
(12) Creighton, J. A.; Blatchford, C. G.; Albrecht, M. G. *J. Chem. Soc., Faraday Trans. 2* **1979**, *75*, 790−798.
(13) Cang, H.; Labno, A.; Lu, C.; Yin, X.; Liu, M.; Gladden, C.; Liu, Y.; Zhang, X. *Nature* **2011**, *469*, 385−388.
(14) Alù, A.; Engheta, N. *Phys. Rev. E* **2005**, *72*, 016623.
(15) Silveririnha, M. G.; Alù, A.; Engheta, N. *Phys. Rev. B.* **2008**, *78*, 075107.
(16) Bohren, C. F.; Huffman, D. R. *Absorption and Scattering of Light by Small Particles*; Wiley: New York, 1983.
(17) Nozawa, K.; Gailhanou, H.; Raison, L.; Panizza, P.; Ushiki, H.; Sellier, E.; Delville, J. P.; Delville, M. H. *Langmuir* **2004**, *21*, 1516−1523.
(18) Martin, M. N.; Basham, J. I.; Chando, P.; Eah, S. K. *Langmuir* **2010**, *26*, 7410−7417.
(19) Turkevich, J.; P.C. Stevenson, J. H. *Discuss. Faraday Soc.* **1951**, *11*, 55−75.
(20) Mulvaney, P. *Langmuir* **1996**, *12*, 788−800.
(21) Pastoriza-Santos, I.; Gomez, D.; Perez-Juste, J.; Liz-Marzán, L. M.; Mulvaney, P. *Phys. Chem. Chem. Phys.* **2004**, *6*, 5056−5060.
(22) Pang, M. L.; Zeng, H. C. *Langmuir* **2010**, *26*, 5963−5970.
(23) Zhang, L.; Wang, H. *ACS Nano* **2011**, *5*, 3257−3267.
(24) Jeong, S.; Woo, K.; Kim, D.; Lim, S.; Kim, J. S.; Shin, H.; Xia, Y.; Moon, J. *Adv. Funct. Mater.* **2008**, *18*, 679−686.
(25) Yin, M.; Wu, C. K.; Lou, Y.; Burda, C.; Koberstein, J. T.; Zhu, Y.; O'Brien, S. *J. Am. Chem. Soc.* **2005**, *127*, 9506−9511.
(26) Malerba, C.; Biccari, F.; Ricardo, C. L. A.; D'Incau, M.; Scardi, P.; Mittiga, A. *Sol. Energy Mater. Sol. Cells* **2011**, *95*, 2848−2854.
(27) Khon, E.; Mereshchenko, A.; Tarnovsky, A. N.; Acharya, K.; Klinkova, A.; Hewa-Kasakarage, N. N.; Nemitz, I.; Zamkov, M. *Nano Lett.* **2011**, *11*, 1792−1799.
(28) Mokari, T.; Rothenberg, E.; Popov, I.; Costi, R.; Banin, U. *Science* **2004**, *304*, 1787−1790.
(29) Myroshnychenko, V.; Rodriguez-Fernandez, J.; Pastoriza-Santos, I.; Funston, A. M.; Novo, C.; Mulvaney, P.; Liz-Marzan, L. M.; Abajo, F. J. G. d. *Chem. Soc. Rev.* **2008**, *37*, 1792−1805.
(30) Johnson, P. B.; Christy, R. W. *Phys. Rev. B* **1972**, *6*, 4370−4379.
(31) Kedem, O.; Vaskevich, A.; Rubinstein, I. *J. Phys. Chem. Lett.* **2011**, *2*, 1223−1226.